Published in final edited form as:
Neuroimage. 2013 February 1; 0: 161–168. doi:10.1016/j.neuroimage.2012.10.014.

Relationship between fractional anisotropy of cerebral white matter and metabolite concentrations measured using ^{1}H magnetic resonance spectroscopy in healthy adults

S.A. Wijtenburg[a,*], **S.A. McGuire**[b], **L.M. Rowland**[a,*], **P.M. Sherman**[c], **J.L. Lancaster**[d], **D.F. Tate**[d], **L.J. Hardies**[d], **B. Patel**[a,f,*], **D.C. Glahn**[e], **L.E. Hong**[a,*], **P.T. Fox**[d], and **P. Kochunov**[a,f,*]

[a]Maryland Psychiatric Research Center, Department of Psychiatry, University of Maryland School of Medicine, Baltimore, MD, USA

[b]Aerospace Medicine Consultation Division, Dayton, OH, USA

[c]Department of Neuroradiology, Wilford Hall Ambulatory Surgical Center, San Antonio, TX, USA

[d]Research Imaging Institute, University of Texas Health Science Center at San Antonio, San Antonio, TX, USA

[e]Department of Psychiatry, Yale University and Olin Neuropsychiatric Research Center, Hartford, CT, USA

[f]Department of Physics, University of Maryland Baltimore County (UMBC), MD, USA

Abstract

Fractional anisotropy (FA) of water diffusion in cerebral white matter (WM), derived from diffusion tensor imaging (DTI), is a sensitive index of microscopic WM integrity. Physiological and metabolic factors that explain intersubject variability in FA values were evaluated in two cohorts of healthy adults of different age spans (N=65, range: 28–50 years; and N=25, age=66.6±6.2, range:57–80 years). Single voxel magnetic resonance spectroscopy (MRS) was used to measure N-acetylaspartate (NAA), total choline-containing compounds, and total creatine, bilaterally in an associative WM tract: anterior corona radiata (ACR). FA values were calculated for the underlying, proximal and two distal WM regions. Two-stage regression analysis was used to calculate the proportion of variability in FA values explained by spectroscopy measurements, at the first stage, and subject's age, at the second stage. WM NAA concentration explained 23% and 66% of intersubject variability ($p<0.001$) in the FA of the underlying WM in the younger and older cohorts, respectively. WM NAA concentration also explained a significant proportion of variability in FA of the genu of corpus callosum (CC), a proximal WM tract where some of the

[*]Neuroimaging Research Program, Maryland Psychiatric Research Center, Department of Psychiatry, University of Maryland School of Medicine, P.O. Box 21247, Baltimore, MD 21228, pkochunov@mprc.umaryland.edu, phone: (410) 402-6110, fax: (410) 402-6077.

Disclosure
Authors have no conflict of interest information to disclose.

fibers contained within the spectroscopic voxel decussate spectroscopic voxel decussate. NAA concentrations also explained a significant proportion of variability in the FA values in the splenium of CC, a distal WM tract that also carries associative fibers, in both cohorts. These results suggest that MRS measurements explained a significant proportion of variability in FA values in both proximal and distal WM tracts that carry similar fiber-types.

Keywords

diffusion tensor imaging; white matter; magnetic resonance spectroscopy; and N-acetylaspartate

1.0 Introduction

Fractional anisotropy (FA) of water diffusion in cerebral white matter (WM) is a neuroimaging index that is commonly used as a measure of microscopic WM integrity (Kamagata et al., 2012; Kochunov et al., 2009; Onu et al., 2012). Absolute FA values are sensitive to many factors including myelin integrity, axonal density, fiber diameter, and the configuration of axonal packing (Hasan et al., 2009; Kochunov et al., 2007; Kochunov et al., 2012; Madler et al., 2008; Minati et al., 2007; Moseley, 2002a; O'Donnell and Westin, 2011; Wozniak and Lim, 2006). Our aim was to examine the neurochemical factors that can potentially explain the individual variability in the frontal FA values. To this end, we studied the correspondence between FA values and concentrations of three important neurochemicals measured with ^{1}H magnetic resonance spectroscopy (^{1}H MRS) in the same frontal WM region. Specifically, we performed regression analyses to estimate the proportion of individual variability in FA values that can be explained by concentrations of N-acetylaspartate (NAA), total choline containing compounds (tCho), and total creatine (tCr) using ^{1}H MRS in two groups of healthy normal volunteers.

FA is measured using diffusion tensor imaging (DTI) to quantify the directional selectivity of the random motion of water molecules within a tissue (Basser, 1994; Conturo et al., 1996; Pierpaoli and Basser, 1996; Ulug et al., 1995). Higher FA values (maximum theoretical value is 1.0) are observed along heavily myelinated WM tracts. The structure of the axonal cell membranes and myelin sheath hinders the diffusion of water molecules in all but the direction along the fiber tract, therefore producing highly anisotropic water diffusion (Pierpaoli and Basser, 1996). As a neuroimaging index of WM integrity, FA offers insight into the changes in the micro-structural integrity of WM tracts. Its ageing and disease related decline is associated with an increase in the water diffusion across the myelin sheath, and is commonly interpreted as evidence for demyelination, reduction in the density of oligodendrocytes and/or replacement of axonal fibers with other cells (Horsfield and Jones, 2002; Smith et al., 2006b; Song et al., 2003; Song et al., 2005).

Here, we chose to study the frontal association WM tract, the anterior corona radiata (ACR). ACR is an associative, cortico-cortical frontal WM tract that decussates in the genu of corpus callosum and relays higher-order cognitive information (Mamata et al., 2002). ACR's FA values experience a precipitous decline in normal aging (Kochunov et al., 2012; Moseley, 2002b; Sullivan et al., 2001) because the oligodendrocytes that myelinate this tract have reduced rates (per axonal-segment) of myelin production and repair (Hof et al., 1990)

and are highly susceptible to metabolic damage (Bartzokis et al., 2004b). We hypothesized that MRS markers will capture a significant proportion of individual variability in the FA values in the underlying WM and the FA values of the proximal WM tracts that carry some of these fibers. To test this hypothesis, we calculated the FA values for the MRS voxel, the anterior corona radiata (ACR), an associative WM tract where the MRS voxel was placed, and the genu of corpus callosum, where ACR fibers decussate. We also hypothesized that MRS markers may explain variability in the FA values for distal WM tracts that do not carry the fibers from where the MRS measurements were derived. To test this hypothesis, we correlated MRS measurements with the FA values for the body of CC, which contains decussating motor and sensory fibers and the splenium of CC where associative fibers that carry visual and spatial-orientation information decussate.

^{1}H-MRS allows for noninvasive concentration measurements of biologically important neurochemicals *in vivo*. The three most commonly reported metabolites are N-acetylaspartate (NAA), total choline containing compounds (tCho), and total creatine (tCr). NAA is an abundant amino acid in the CNS that is highly concentrated in neuronal bodies and axons (Govindaraju et al., 2000; Moffett et al., 2007), and its concentration is often used as a marker of neuronal viability (Cecil and Kos, 2006; Govindaraju et al., 2000). It plays an important role in osmoregulation (Baslow, 2003a, b, 2010) and participates in the synthesis of myelin through donation of its acetate group (Baslow, 2003b; Moffett et al., 2007). In previous studies of aging and ^{1}H-MRS, NAA concentrations in frontal white matter regions remain steady or decline as a function of age (Chang et al., 1996; Chang et al., 2009). Decline in the NAA concentration is also observed in ischemic stroke and is interpreted as a loss of viable neurons (Munoz Maniega et al., 2008). When measured WM, NAA concentrations showed a strong correlation with axonal density in postmortem human MS lesions, suggesting that NAA is a strong indicator of axonal integrity (Bjartmar et al., 2000). The dominant tCho resonance is made up of glycerophosphocholine, a product of cellular membrane breakdown, and phosphocholine, a cellular membrane precursor (Cecil and Kos, 2006). In normal aging, tCho concentrations in frontal white matter remain stable or increase as a function of age (Chang et al., 1996; Chang et al., 2009). Increased tCho concentrations are commonly interpreted as a breakdown in cellular membranes (Klein, 2000). In a study of brain tumors, resected cerebral tissue with elevated tCho concentration *in vivo* showed evidence for cellular inflammation (Venkatesh et al., 2001). Elevated tCho concentration was observed in Alzheimer's disease, potentially indicating increased membrane turnover due to neurodegeneration (Kantarci, 2007). Finally, the tCr signal, made up of creatine and phosphocreatine, is a measurement of compensatory energy metabolism activity (Balestrino et al., 2002; Govindaraju et al., 2000). Once thought to be stable across development and disease states, tCr concentration was commonly used as an internal reference for other metabolites in the spectrum. However, more recent studies on healthy aging have reported that in tCr concentrations in cerebral WM may decline with age and this change indicates compromised energy metabolism (Chang et al., 1996; Chang et al., 2009). When lacking glucose or oxygen, tCr concentrations partially offset the energy deficits from impaired ATP production, but the supply of tCr is limited. Thus, a marked decrease in tCr concentration suggests impaired energy metabolism (Balestrino et al., 2002). Recent research also showed that tCr can be altered in pathological states (Pilatus et al., 2009; van den Bogaard et al.,

2011), and this putatively reflects metabolic alterations. For instance, decline in tCr concentrations was reported in asymptomatic subjects with a genetic predisposition to Huntington's disease (van den Bogaard et al., 2011). In a study of mild cognitive impairment (MCI), Pilatus and colleagues found significantly decreased tCr was predictive of subjects who converted to dementia during the next follow-up (Pilatus et al., 2009).

In this study, we carefully examined FA values and concentrations of ^{1}H MRS markers in the younger (3rd-to-5th decades) and older-age cohorts (6th-to-8th decades). FA values follow an inverted-U trajectory with age that peaks in the 3rd–4th decades of life (Figure 1). As such, the two cohorts corresponded to the periods of small (young age cohort) and large (old age cohort) expected age-related change in FA values (Figure 1). We focused on examining the degree of intersubject variability in FA values that can be explained by differences in the concentrations of biologically important neurochemicals derived from the proximal WM region as well as from two more distal WM regions one that carried similar, associative fibers and the other that carried motor and sensory fibers. Additionally, we examined potential differences in the relationship between spectroscopic measurements and FA values in populations at the different stages of their lifelong FA trajectory. We hypothesized that NAA concentration would be strongly correlated with FA values, and that this relationship will be significant for both cohorts. Together, the relationships between FA and the three neurochemicals clarified the nature of the intersubject differences in FA as well as the physiological differences between younger and older age subjects.

2.0 Material and Methods

All studies were performed at the Research Imaging Institute, University of Texas Health Science Center at San Antonio. DTI and MRS data for 65 healthy, younger-age male participants (mean age: 37.4 ± 6.0, range: 28–50 years) were collected using Siemens Tim Trio 3T MR system (Erlangen, Germany) using a twelve-channel head coil. Similar data were collected for 25 healthy older-age participants (mean age: 66.6 ± 6.2, range: 57–80 years, 8 males and 17 females) using Siemens Trio 3T MR system. For the older-age group, an eight-channel phase array coil was used for collection of DTI data while a transmit-receive quadrature head coil was used for collection of the ^{1}H MRS data. The imaging protocol consisted of a high-resolution diffusion tensor imaging, a 3-D 1-mm^{3} turbo-spin-echo FLAIR sequence, and a single voxel PRESS spectroscopy sequence (Bottomley, 1987). The following measurements were performed in both cohorts: 1) FA values for the spectroscopic region-of-interest (sROI) corresponding to the spectroscopic voxel, the anterior corona radiata (ACR), and the genu of the corpus callosum; and 2) spectroscopic metabolite concentrations including NAA, tCr (creatine+phosphocreatine), and tCho (glycerophosphocholine+phosphocholine) in the frontal WM regions.

2.1 Diffusion tensor imaging

A single-shot, echo-planar, single refocusing spin-echo sequence was used to acquire diffusion-weighted data with a spatial resolution of 1.7×1.7×3.0-mm in both cohorts. The same sequence parameters were: TE/TR=87/8000ms, FOV=200mm, two diffusion weighing values b=0 and 700 s/mm^{2} and three b=0 (non-diffusion weighted) images, axial slice orientation with 50 slices and no gaps. A single average was used in both studies. The data

for younger age subjects were collected with 55 isotropically distributed diffusion weighted directions, while the DTI data for older subjects were collected using 86 isotropically distributed diffusion directions. The number of directions, b=0 images, and the magnitude of the b values for each protocol were calculated using an optimization technique that maximizes the contrast to noise ratio based on the average diffusivity of the cerebral WM and the T_2 relaxation times (Jones et al., 1999). The higher number of directions in the older cohort was used to increase the signal-to-noise ratio because the eight-channel coil produced weaker signal than the twelve-channel coil used in the younger cohort.

2.2 Processing of DTI data

Fractional anisotropy (FA) images were created by fitting the diffusion tensor to the raw diffusion data (Smith SM, 2002). The DTI data were processed in two ways. First, the average FA value was calculated from the spectroscopic region of interest that was placed on the FA image. Next, the average FA values for the spectroscopic voxel as well as two proximal (anterior corona radiate and the genu of corpus callosum) and two distal (body and splenium of corpus callosum) WM tracts were calculated using a tract-based spatial statistics (TBSS) analytic method, distributed as a part of FMRIB Software Library (FSL) package, was used for tract-based analysis of diffusion anisotropy (Smith et al., 2006a; Smith et al., 2007). The TBSS approach was developed to overcome the limitations of voxel and region-of-interest (ROI) based analysis of DTI data. FA images are characterized by a steep drop-off in the magnitude of FA values in the direction that is perpendicular to the principle direction of the tract. Therefore, FA images are typically inadequate for intersubject voxel-based analysis and ROI-based analyses because the steep gradients in regional intensity can produce misalignment and partial-volume averaging effects (Smith et al., 2006b). The TBSS combines the strengths of voxel-wise (e.g., VBM - voxel based morphometry(Ashburner and Friston, 2000)) statistical analysis and WM tractography methods by extracting the spatial course of major WM tracts and then analyzing the FA values that correspond to the middle of the tract.

During TBSS processing, all FA images were globally spatially normalized and then nonlinearly aligned to a group-wise, minimal-deformation target (MDT) brain. The global spatial normalization was performed using a method distributed with FSL package (FLIRT) (Smith et al., 2006a) with 12 degrees of freedom. This step was performed to reduce the global intersubject variability in brain volumes prior to non-linear alignment. The group's MDT brain is identified by warping all individual brain images in the group to each brain (Kochunov et al., 2001). The MDT is selected as the image that minimizes the amount of the required deformation from other images in the group. Next, individual FA images are averaged to produce a group-average anisotropy image. This image is used to create a group-wise skeleton of WM tracts. The skeletonization procedure is a morphological operation, which extracts the medial axis of an object. This procedure is used to encode the medial trajectory of the WM fiber-tracts with one-voxel thin sheaths. Finally, FA values from each image are projected onto the group-wise skeleton of WM structures. This step accounts for residual misalignment among individual WM tracts. FA values are assigned to each point along a skeleton using the peak value found within a designated range perpendicular to the skeleton. The FA values vary rapidly perpendicular to the tract direction

but very slowly along the tract direction. By assigning the peak value to the skeleton, this procedure effectively maps the center of individual WM tracts on the skeleton. This processing is performed under two constraints. A distance map is used to establish search borders for individual tracts. The borders are created by equally dividing the distance between two nearby tracts. Secondly, a multiplicative 20mm full width at half-max Gaussian weighting is applied during the search to limit maximum projection distance from the skeleton.

2.3 Tract-based analysis using JHU atlas

The population-based, 3D, DTI cerebral WM tract atlas developed in Johns Hopkins University (JHU) and distributed with the FSL package (Wakana et al., 2004) was used to calculate population average FA values along the spatial course of the two WM tracts that were proximal to sROI: the ACR and the genu of corpus callosum (CC). Both of these tracts contained the decussating associative fibers localized within the MRS voxel (Figure 2). Additionally, we calculated the average FA values for the two distal WM tracts: the body and splenium of CC (Figure 2). The CC is the largest commissural projection system in the CNS. We chose to study it here because histological examinations have demonstrated that the CC is composed of distinct fiber types (Aboitiz, 1992; Aboitiz et al., 1992; Lamantia and Rakic, 1990; Witelson, 1989). The genu (anterior third of the CC) mainly contains the thinly myelinated and unmyelinated associative fibers that connect the bilateral prefrontal cortices. The body (middle third) primarily contains heavily myelinated commissural fibers for motor, somatosensory and auditory cortices. The splenium (posterior third) carries thickly myelinated commissural fibers, intermixed with thinly myelinated associative fibers that connect the temporal, parietal and occipital lobes (Aboitiz, 1992; Aboitiz et al., 1992; Lamantia and Rakic, 1990; Witelson, 1989). The per-tract average values were calculated by averaging the values along the tracts in both hemispheres.

2.4 Spectroscopy

Single voxel PRESS localization was utilized with the following parameters: TR/TE = 1500/135-ms, VOI ~ 3.4-cm3, NEX = 256, 1024 complex points, 1.2k-Hz spectral width, and total scan time ~ 12 minutes. A water reference (NEX = 4) was collected and utilized for phasing and eddy current correction. Spectroscopic voxels were placed bilaterally in the white matter of the forceps minor area of each hemisphere in order to prevent partial volume averaging with CSF and gray matter (Figure 2). Both datasets were collected by the same technician who ensured the correct placement of the spectroscopic voxel in pure white matter. The post-hoc analysis using tissue segmented images in the young cohort was used to verify that 99% of the voxel within the region of spectroscopy measurements contained >95% WM in all of the subjects. The intersubject overlap of the spectroscopic voxel is shown for young subjects, following normalization to the Talairach frame in Figure 1S, see supplement. This analysis could not be performed in the older cohort because the spectroscopy and anatomical data were collected using different head coils, resulted in the loss of the isocenter location between two acquisitions.

All data were phased and apodized to improve the signal-to-noise ratio (SNR) using an in-house IDL program (Exelis Visual Information Solutions, Inc, Boulder, CO, USA)

(Wijtenburg and Knight-Scott, 2011). The basis set was simulated using the GAVA software package (Soher et al., 2007), which was modified to yield a Lorentzian lineshape instead of its default Gaussian lineshape. The basis set was made up of: creatine (Cr), glycerophosphocholine (GPC), lactate (Lac), myo-Inositol (mI), N-acetylaspartate (NAA), N-acetylaspartylglutamate (NAAG), phosphocholine (PCh), and phosphocreatine (PCr). This basis set was imported into LCModel, a fully automated curve fitting software package (Provencher, 1993) for metabolite quantification. All metabolite concentrations were relative to the water reference and therefore reported in institutional units (IU). Metabolite fits with Cramer Rao Lower Bounds (CRLBs) above 20% were excluded (N=3, all in elderly cohort).

2.5 Statistics

A two-stage linear regression was used to probe the multivariate effects of the three ^{1}H-MRS measurements and intersubject variability in FA values. MRS measurements were entered at the first stage, and subject's age was entered at the second stage to estimate the unexplained residual variability. The regression analysis yielded the degree of variance described at each entry step and whether the change was significant. It also produced standardized coefficients (β) that estimate linear associations between FA measurements (the criterion) and biochemical indices of cerebral integrity (the predictors). This analysis was performed separately for the three (sROI, ACR, and the genu of corpus callosum) regional FA values for each of the cohorts. We corrected for multiple comparisons using Bonferroni correction (N=3) such that significance was set to $p < 0.017$.

Results

3.1 Young-Age Cohort

Means for regional FA values and metabolite concentrations are shown in Table 1. In each of the regions, the only significant predictor of FA value was NAA concentration (Table 2). The strongest effect was observed for FA values in the sROI calculated using the TBSS approach ($r^2 = 0.23$, $p = 0.0001$, Figure 3), followed by the corpus callosum and ACR ($r^2 = 0.22$, 21 $p < 0.001$, respectively). The correlation between FA values in the sROI calculated from raw FA maps was weak but significant ($r^2 = 0.12$, $p = 0.01$)

Analysis for the two distal WM tracts demonstrated that NAA from the associative frontal WM fibers demonstrated a significant relationship with the FA of the visual and spatial orientation fibers of the splenium of CC and with the motor and sensory fibers located in the body of CC ($r^2 = 0.22$ and 0.21 and $p<0.01$, respectively) (Table 3).

3.2 Old-Age Cohort

A summary of FA values and metabolite concentrations in each region are shown in Table 4. Similarly to the young cohort, the strongest association was observed between NAA and FA values in the sROI calculated from TBSS data ($r^2 = 0.66$, $p < 0.001$, Figure 3, Table 5). The associations between NAA and the average sROI FA value calculated from the raw FA images was weaker, but still highly significant ($r^2 = 0.34$, $p = 0.002$). A similar pattern of significant prediction by NAA was observed in the ACR ($r^2 = 0.56$, $p = 0.0001$) and to a lesser extent in the genu ($r^2 = 0.28$, $p = 0.01$).

Similarly, the analysis for the two distal WM tracts, in the old-age cohort demonstrated, that NAA measurement from the associative frontal WM fibers predicted a significant relationship ($r^2 = 0.13$, $p=0.047$) with the FA of the visual and spatial orientation fibers of the splenium of CC (Table 6). The relationship with the FA values of body of CC was not significant (Table 6).

Discussion

To our knowledge this is the first study to systematically demonstrate and replicate the relationship between FA values and metabolite concentrations in the underlying, proximal and distal WM fibers. We observed that NAA concentrations predict a highly significant degree of the variance in the underlying FA values in both young and old-age cohorts. In the younger age group, the observed predictive power was nearly equivalent for the sROI, anterior corona radiata (ACR) and the genu of corpus callosum (CC). In the older-age cohort, the relationship between NAA and FA was more prominent but also more regional. There, the NAA concentrations explained 66% of the variance in FA values within the sROI but the predictive power dropped to 56% for the ACR and 28% for the genu of CC. Nonetheless, the correlation between NAA and the FA values for the underlying and proximal WM were independently significant in each cohort even after Bonferroni corrections. Analysis of the FA values for the WM areas distal to the spectroscopic voxel suggested that NAA levels measured in frontal associative WM were also predictive of FA values in the splenium of CC in both cohorts. Splenium carries associative fibers that connect parietal areas (Aboitiz, 1992; Aboitiz et al., 1992). The correlation between NAA and FA values of the body of CC was only significant in the younger-age cohort. This suggested that NAA measurements in frontal WM were predictive of the aging trends experienced by WM regions that carried fibers of a similar architecture

This study also demonstrated the superiority of using TBSS approach over the region-of-interest data for multisubject analysis. The correlation between NAA and the average FA value calculated from TBSS skeletons was stronger than those calculated by voxel-wise averaging of FA maps and this finding was expected. TBSS offers the advantage of projecting tract center values onto the mean FA skeleton. This approach ensures that an equivalent set of voxels is included from each subject. This is very important given the steep drop-off in FA values in the direction that is perpendicular to the tract's principle direction where partial voxel averaging dependent of the ROI placement can introduce extra variability (Smith et al., 2006a; Smith et al., 2004). Overall, these results support our hypothesis that MRS measurement can be insightful to understanding intersubject variability of FA values throughout the lifespan. These results also suggest that MRS measurements in frontal associative WM can predict variability in FA values in the distal WM tracts that carry associative fibers.

NAA concentrations were strongly and positively correlated with the underlying FA values in both cohorts. The magnitude of the correlation coefficient was larger in the older age cohort ($r = 0.81$) than the younger age cohort ($r = 0.46$) and this difference was statistically significant ($Z=\sim-2.5$; $p<0.01$). The NAA signal derived from pure cerebral WM reflects NAA concentrations in axons and therefore is considered a marker of neuronal axonal

health. Conversely, intersubject variability in regional FA values is predominantly explained (~80–90%) by differences in the myelin levels and therefore reflect the viability of the oligodendrocytes which myelinate CNS axons (Madler et al., 2008; Song et al., 2003). One of NAA's many physiological roles is in the maintenance of cerebral myelination. NAA is thought to be transferred from axons to oligodendrocytes where its acetate moiety is removed and utilized for myelin synthesis (Moffett et al., 2007). The strong correlation between FA values and NAA concentrations suggests a potential mechanism for age-related alterations in FA values commonly reported in the literature (Hasan et al., 2009; Kochunov et al., 2007; Kochunov et al., 2012; Minati et al., 2007; Moseley, 2002b).

Our finding of a strong and a positive relationship between NAA concentrations and the FA of the WM fibers suggests two possible scenarios: neuronal and glial. NAA is produced in neuronal mitochondria and is a marker of neuronal function (Baslow, 2003b) and neuronal density (Bjartmar et al., 2002). A decline in cortical NAA concentration observed with age and or a disorder is considered to be the result of the loss in the neuronal number or function (Bjartmar et al., 2002). The decline in cortical neuronal density in associative areas would inevitably lead to reduction in axonal density in the WM tracts that interconnect them. Therefore, the decline in WM NAA concentrations may reflect on the age-related loss in cortical neuronal density and the corresponding loss in axonal numbers leads to decline in FA values due to the axonal degeneration and demyelination. Alternatively, aging-related loss in glial cell density may lead to demyelination and loss of axonal fibers or function, resulting in lower FA values and NAA levels. This could explain why NAA measurements from associative frontal areas were also significantly correlated with the FA values in the distal WM fibers that carry associative but not sensory and motor information. Oligodendrocytes that myelinate these associative WM tracks are among the most metabolically active cells in the adult CNS and therefore vulnerable to accumulation of metabolic damage (Bartzokis et al., 2001; Bartzokis et al., 2003; Bartzokis et al., 2004a). This damage leads to axonal loss, which adversely affects the neurons throughout the cortex due to loss of neurotrophic factors (Dai et al., 2001; Wilkins et al., 2001; Wilkins et al., 2003). However, additional investigations that take into account the cortical neuronal density measured either by cortical NAA concentrations or cortical gray matter thickness are needed to test these hypotheses. Additionally, short echo time 1H-MRS sequences can be used to calculate the concentrations of other metabolites such as myo-inositol, a marker of glial cell density, to aid in understanding of physiological mechanisms behind decreased FA values with age.

This study calculated the concentrations of the metabolically important neurochemicals in part-per-million using the water peak as the reference value. Historically, the concentrations for NAA and tCho were also reported as a ratio to the concentrations of tCr because this did not require collection of the water reference data. The concentration of tCr was assumed to be stable across age and disorders, however, this assumption was inaccurate according to recent data (Chang et al., 1996; Chang et al., 2009). When referenced to tCr level, the relationship between NAA and underlying FA values was weaker, albeit this difference was not statistically significant (r^2= 0.08 vs 0.21, z=−1.1, p=0.20 and r^2=0.27 vs.0.65, z=−1.74, p=0.08 for the young and old cohort respectively). A similar reduction in significance was observed by a study that evaluated the genetic portion of the individual variability in MRS

measurements in a large twin sample (Batouli et al., 2012). There, the concentrations of NAA and tCho demonstrated significantly higher heritability, with up to 65% of the variance in NAA explained by genetic factors, when referenced to water rather than tCr level due to lower environmental variance(Batouli et al., 2012). They concluded that “strong environmental influences on tCr level suggests that it cannot be the best internal reference” and that “the heritability of the metabolites considerably reduced when tCr was used as the reference, and therefore our data suggest that the unsuppressed water peak may be the more appropriate reference”(Batouli et al., 2012).

A limitation of this study is that the data for two groups were acquired using different scanners and head coils. This prevented the combined analysis of the overall effects of FA values and metabolite concentration as a function of aging. Another limitation of this study is that there were no corrections for tissue water content in the metabolite concentrations. Tissue water content has been shown to decrease as a function age (Chang et al., 1996; Haley et al., 2004), which would result in higher metabolite concentrations in the elderly group and potentially affect our analyses.

Supplementary Material

Refer to Web version on PubMed Central for supplementary material.

Acknowledgments

This research was supported by a United States Air Force Surgeon General grant (Log I-11-44) to Dr. McGuire, T32 MH067533 to Dr. Wijtenburg, K01 MH077230 to Dr. Rowland and K01 EB006395 and R01 EB015611 to Dr. Kochunov. Research support was also provided National Institute of Mental Health (RO1s MH078111, MH0708143 and MH083824) to Dr. Glahn and by the Human Brain Mapping Project, which is jointly funded by NIMH and NIDA (P20 MH/DA52176). This research was also supported, in part, by an Undergraduate Research Assistantship award to PB from the UMBC Office of Research Administration.

References

Aboitiz F. Brain connections: interhemispheric fiber systems and anatomical brain asymmetries in humans. Biol Res. 1992; 25:51–61. [PubMed: 1365702]

Aboitiz F, Scheibel AB, Fisher RS, Zaidel E. Fiber composition of the human corpus callosum. Brain Res. 1992; 598:143–153. [PubMed: 1486477]

Ashburner J, Friston KJ. Voxel-based morphometry--the methods. Neuroimage. 2000; 11:805–821. [PubMed: 10860804]

Balestrino M, Lensman M, Parodi M, Perasso L, Rebaudo R, Melani R, Polenov S, Cupello A. Role of creatine and phosphocreatine in neuronal protection from anoxic and ischemic damage. Amino Acids. 2002; 23:221–229. [PubMed: 12373542]

Bartzokis G, Beckson M, Lu PH, Nuechterlein KH, Edwards N, Mintz J. Age-related changes in frontal and temporal lobe volumes in men: a magnetic resonance imaging study. Arch Gen Psychiatry. 2001; 58:461–465. [PubMed: 11343525]

Bartzokis G, Cummings JL, Sultzer D, Henderson VW, Nuechterlein KH, Mintz J. White matter structural integrity in healthy aging adults and patients with Alzheimer disease: a magnetic resonance imaging study. Arch Neurol. 2003; 60:393–398. [PubMed: 12633151]

Bartzokis G, Sultzer D, Lu PH, Nuechterlein KH, Mintz J, Cummings J. Heterogeneous age-related breakdown of white matter structural integrity: Implications for cortical “disconnection” in aging and Alzheimer’s disease. Neurobiol Aging. 2004a; 25:843–851. [PubMed: 15212838]

Bartzokis G, Sultzer D, Lu PH, Nuechterlein KH, Mintz J, Cummings JL. Heterogeneous age-related breakdown of white matter structural integrity: implications for cortical “disconnection” in aging and Alzheimer’s disease. Neurobiol Aging. 2004b; 25:843–851. [PubMed: 15212838]

Baslow MH. Brain N-acetylaspartate as a molecular water pump and its role in the etiology of Canavan disease: a mechanistic explanation. J Mol Neurosci. 2003a; 21:185–190. [PubMed: 14645985]

Baslow MH. N-acetylaspartate in the vertebrate brain: metabolism and function. Neurochem Res. 2003b; 28:941–953. [PubMed: 12718449]

Baslow MH. Evidence that the tri-cellular metabolism of N-acetylaspartate functions as the brain’s “operating system”: how NAA metabolism supports meaningful intercellular frequency-encoded communications. Amino Acids. 2010; 39:1139–1145. [PubMed: 20563610]

Basser PJ. Focal magnetic stimulation of an axon. IEEE Transactions on Biomedical Engineering. 1994; 41:601–606. [PubMed: 7927380]

Batouli SA, Sachdev PS, Wen W, Wright MJ, Suo C, Ames D, Trollor JN. The heritability of brain metabolites on proton magnetic resonance spectroscopy in older individuals. Neuroimage. 2012; 62:281–289. [PubMed: 22561359]

Bjartmar C, Battistuta J, Terada N, Dupree E, Trapp BD. N-acetylaspartate is an axon-specific marker of mature white matter in vivo: a biochemical and immunohistochemical study on the rat optic nerve. Ann Neurol. 2002; 51:51–58. [PubMed: 11782984]

Bjartmar C, Kidd G, Mork S, Rudick R, Trapp BD. Neurological disability correlates with spinal cord axonal loss and reduced N-acetyl aspartate in chronic multiple sclerosis patients. Ann Neurol. 2000; 48:893–901. [PubMed: 11117546]

Bottomley PA. Spatial localization in NMR spectroscopy in vivo. Ann N Y Acad Sci. 1987; 508:333–348. [PubMed: 3326459]

Cecil KM, Kos RS. Magnetic resonance spectroscopy and metabolic imaging in white matter diseases and pediatric disorders. Top Magn Reson Imaging. 2006; 17:275–293. [PubMed: 17415001]

Chang L, Ernst T, Poland RE, Jenden DJ. In vivo proton magnetic resonance spectroscopy of the normal aging human brain. Life Sci. 1996; 58:2049–2056. [PubMed: 8637436]

Chang L, Jiang CS, Ernst T. Effects of age and sex on brain glutamate and other metabolites. Magn Reson Imaging. 2009; 27:142–145. [PubMed: 18687554]

Conturo TE, McKinstry RC, Akbudak E, Robinson BH. Encoding of anisotropic diffusion with tetrahedral gradients: a general mathematical diffusion formalism and experimental results. Magn Reson Med. 1996; 35:399–412. [PubMed: 8699953]

Dai X, Qu P, Dreyfus CF. Neuronal signals regulate neurotrophin expression in oligodendrocytes of the basal forebrain. Glia. 2001; 34:234–239. [PubMed: 11329185]

Govindaraju V, Young K, Maudsley AA. Proton NMR chemical shifts and coupling constants for brain metabolites. NMR Biomed. 2000; 13:129–153. [PubMed: 10861994]

Haley AP, Knight-Scott J, Fuchs KL, Simnad VI, Manning CA. Shortening of hippocampal spin-spin relaxation time in probable Alzheimer’s disease: a 1H magnetic resonance spectroscopy study. Neurosci Lett. 2004; 362:167–170. [PubMed: 15158006]

Hasan KM, Kamali A, Iftikhar A, Kramer LA, Papanicolaou AC, Fletcher JM, Ewing-Cobbs L. Diffusion tensor tractography quantification of the human corpus callosum fiber pathways across the lifespan. Brain Res. 2009; 1249:91–100. [PubMed: 18996095]

Hof PR, Cox K, Morrison JH. Quantitative analysis of a vulnerable subset of pyramidal neurons in Alzheimer’s disease: I. Superior frontal and inferior temporal cortex. J Comp Neurol. 1990; 301:44–54. [PubMed: 2127598]

Horsfield MA, Jones DK. Applications of diffusion-weighted and diffusion tensor MRI to white matter diseases - a review. NMR Biomed. 2002; 15:570–577. [PubMed: 12489103]

Jones DK, Horsfield MA, Simmons A. Optimal strategies for measuring diffusion in anisotropic systems by magnetic resonance imaging. Magn Reson Med. 1999; 42:515–525. [PubMed: 10467296]

Kamagata K, Motoi Y, Abe O, Shimoji K, Hori M, Nakanishi A, Sano T, Kuwatsuru R, Aoki S, Hattori N. White Matter Alteration of the Cingulum in Parkinson Disease with and without

Dementia: Evaluation by Diffusion Tensor Tract-Specific Analysis. AJNR Am J Neuroradiol. 2012

Kantarci K. 1H magnetic resonance spectroscopy in dementia. Br J Radiol. 2007; 80(Spec No 2):S146–152. [PubMed: 18445744]

Klein J. Membrane breakdown in acute and chronic neurodegeneration: focus on choline-containing phospholipids. J Neural Transm. 2000; 107:1027–1063. [PubMed: 11041281]

Kochunov P, Glahn D, Winkler A, Duggirala R, Olvera RL, Cole S, Dyer TD, Almasy L, Fox PT, Blangero J. Analysis of genetic variability and whole genome linkage of whole-brain, subcortical, and ependymal hyperintense white matter volume. Stroke. 2009; 40:3685–3690. [PubMed: 19834011]

Kochunov P, Lancaster JL, Thompson P, Woods R, Mazziotta J, Hardies J, Fox P. Regional spatial normalization: toward an optimal target. J Comput Assist Tomogr. 2001; 25:805–816. [PubMed: 11584245]

Kochunov P, Thompson PM, Lancaster JL, Bartzokis G, Smith S, Coyle T, Royall DR, Laird A, Fox PT. Relationship between white matter fractional anisotropy and other indices of cerebral health in normal aging: tract-based spatial statistics study of aging. Neuroimage. 2007; 35:478–487. [PubMed: 17292629]

Kochunov P, Williamson DE, Lancaster J, Fox P, Cornell J, Blangero J, Glahn DC. Fractional anisotropy of water diffusion in cerebral white matter across the lifespan. Neurobiol Aging. 2012; 33:9–20. [PubMed: 20122755]

Lamantia AS, Rakic P. Cytological and quantitative characteristics of four cerebral commissures in the rhesus monkey. J Comp Neurol. 1990; 291:520–537. [PubMed: 2329189]

Madler B, Drabycz SA, Kolind SH, Whittall KP, MacKay AL. Is diffusion anisotropy an accurate monitor of myelination? Correlation of multicomponent T2 relaxation and diffusion tensor anisotropy in human brain. Magn Reson Imaging. 2008; 26:874–888. [PubMed: 18524521]

Mamata H, Mamata Y, Westin CF, Shenton ME, Kikinis R, Jolesz FA, Maier SE. High-resolution line scan diffusion tensor MR imaging of white matter fiber tract anatomy. AJNR Am J Neuroradiol. 2002; 23:67–75. [PubMed: 11827877]

Minati L, Grisoli M, Bruzzone MG. MR spectroscopy, functional MRI, and diffusion-tensor imaging in the aging brain: a conceptual review. J Geriatr Psychiatry Neurol. 2007; 20:3–21. [PubMed: 17341766]

Moffett JR, Ross B, Arun P, Madhavarao CN, Namboodiri AM. N-Acetylaspartate in the CNS: from neurodiagnostics to neurobiology. Prog Neurobiol. 2007; 81:89–131. [PubMed: 17275978]

Moseley M. Diffusion tensor imaging and aging - a review. NMR Biomed. 2002a; 15:553–560. [PubMed: 12489101]

Moseley M. Diffusion tensor imaging and aging - a review. NMR Biomed. 2002b; 15:553–560. [PubMed: 12489101]

Munoz Maniega S, Cvoro V, Chappell FM, Armitage PA, Marshall I, Bastin ME, Wardlaw JM. Changes in NAA and lactate following ischemic stroke: a serial MR spectroscopic imaging study. Neurology. 2008; 71:1993–1999. [PubMed: 19064881]

O'Donnell LJ, Westin CF. An introduction to diffusion tensor image analysis. Neurosurg Clin N Am. 2011; 22:185–196. viii. [PubMed: 21435570]

Onu M, Roceanu A, Sboto-Frankenstein U, Bendic R, Tarta E, Preoteasa F, Bajenaru O. Diffusion abnormality maps in demyelinating disease: Correlations with clinical scores. Eur J Radiol. 2012

Pierpaoli C, Basser PJ. Toward a quantitative assessment of diffusion anisotropy. Magn Reson Med. 1996; 36:893–906. [PubMed: 8946355]

Pilatus U, Lais C, Rochmont Adu M, Kratzsch T, Frolich L, Maurer K, Zanella FE, Lanfermann H, Pantel J. Conversion to dementia in mild cognitive impairment is associated with decline of N-actylaspartate and creatine as revealed by magnetic resonance spectroscopy. Psychiatry Res. 2009; 173:1–7. [PubMed: 19427767]

Smith SM. Fast robust automated brain extraction. Hum Brain Mapp. 2002; 17:143–155. [PubMed: 12391568]

Smith SM, Jenkinson M, Johansen-Berg H, Rueckert D, Nichols TE, Mackay CE, Watkins KE, Ciccarelli O, Cader MZ, Matthews PM, Behrens TE. Tract-based spatial statistics: Voxelwise analysis of multi-subject diffusion data. Neuroimage. 2006a; 31:1487–1505. [PubMed: 16624579]

Smith SM, Jenkinson M, Johansen-Berg H, Rueckert D, Nichols TE, Mackay CE, Watkins KE, Ciccarelli O, Cader MZ, Matthews PM, Behrens TE. Tract-based spatial statistics: Voxelwise analysis of multi-subject diffusion data. Neuroimage. 2006b

Smith SM, Jenkinson M, Woolrich MW, Beckmann CF, Behrens TE, Johansen-Berg H, Bannister PR, De Luca M, Drobnjak I, Flitney DE, Niazy RK, Saunders J, Vickers J, Zhang Y, De Stefano N, Brady JM, Matthews PM. Advances in functional and structural MR image analysis and implementation as FSL. Neuroimage. 2004; 23(Suppl 1):S208–219. [PubMed: 15501092]

Smith SM, Johansen-Berg H, Jenkinson M, Rueckert D, Nichols TE, Miller KL, Robson MD, Jones DK, Klein JC, Bartsch AJ, Behrens TE. Acquisition and voxelwise analysis of multi-subject diffusion data with tract-based spatial statistics. Nat Protoc. 2007; 2:499–503. [PubMed: 17406613]

Song SK, Sun SW, Ju WK, Lin SJ, Cross AH, Neufeld AH. Diffusion tensor imaging detects and differentiates axon and myelin degeneration in mouse optic nerve after retinal ischemia. Neuroimage. 2003; 20:1714–1722. [PubMed: 14642481]

Song SK, Yoshino J, Le TQ, Lin SJ, Sun SW, Cross AH, Armstrong RC. Demyelination increases radial diffusivity in corpus callosum of mouse brain. Neuroimage. 2005; 26:132–140. [PubMed: 15862213]

Sullivan EV, Adalsteinsson E, Hedehus M, Ju C, Moseley M, Lim KO, Pfefferbaum A. Equivalent disruption of regional white matter microstructure in ageing healthy men and women. Neuroreport. 2001; 12:99–104. [PubMed: 11201100]

Ulug AM, Barker PB, van Zijl PC. Correction of motional artifacts in diffusion-weighted images using a reference phase map. Magn Reson Med. 1995; 34:476–480. [PubMed: 7500889]

van den Bogaard S, Dumas E, Teeuwisse W, Kan H, Webb A, Roos R, van der Grond J. Exploratory 7-Tesla magnetic resonance spectroscopy in Huntington's disease provides in vivo evidence for impaired energy metabolism. J Neurol. 2011; 258:2230–2239. [PubMed: 21614431]

Venkatesh SK, Gupta RK, Pal L, Husain N, Husain M. Spectroscopic increase in choline signal is a nonspecific marker for differentiation of infective/inflammatory from neoplastic lesions of the brain. J Magn Reson Imaging. 2001; 14:8–15. [PubMed: 11436208]

Wakana S, Jiang H, Nagae-Poetscher LM, van Zijl PC, Mori S. Fiber tract-based atlas of human white matter anatomy. Radiology. 2004; 230:77–87. [PubMed: 14645885]

Wijtenburg SA, Knight-Scott J. Very short echo time improves the precision of glutamate detection at 3T in (1) H magnetic resonance spectroscopy. J Magn Reson Imaging. 2011

Wilkins A, Chandran S, Compston A. A role for oligodendrocyte-derived IGF-1 in trophic support of cortical neurons. Glia. 2001; 36:48–57. [PubMed: 11571783]

Wilkins A, Majed H, Layfield R, Compston A, Chandran S. Oligodendrocytes promote neuronal survival and axonal length by distinct intracellular mechanisms: a novel role for oligodendrocyte-derived glial cell line-derived neurotrophic factor. J Neurosci. 2003; 23:4967–4974. [PubMed: 12832519]

Witelson SF. Hand and sex differences in the isthmus and genu of the human corpus callosum. A postmortem morphological study. Brain. 1989; 112 (Pt 3):799–835. [PubMed: 2731030]

Wozniak JR, Lim KO. Advances in white matter imaging: a review of in vivo magnetic resonance methodologies and their applicability to the study of development and aging. Neurosci Biobehav Rev. 2006; 30:762–774. [PubMed: 16890990]

Highlights

- Fractional anisotropy and concentrations important metabolites were evaluated in two groups of subjects
- In both groups N-acetylaspartate (NAA), a marker of axonal density, predicted variability in FA
- NAA explained 20% of variability in FA in younger and 60% in older subjects
- Decline in NAA can be a potential contributor to the age-related decline in FA values
- This mechanism sheds light on the physiology of aging processes in axons and glial cells

Figure 1.

The age-trends for the two subject groups are overlaid on the average FA values (●) for anterior corona radiata (ACR) tract based on data reported in Kochunov et al., 2012. The two cohorts selected for this study represent two distinct types of aging: young subjects were characterized by a subtle decline in the FA values with age (squares, dotted line, slope= −0.0009 FA/year, r=0.24, p=0.25) and old subjects were characterized by a nearly doubled rate of age-related decline in FA values (circles, dashed line, slope=−0.0017 FA/year, r=0.36, p=0.05). **These data were collected on different scanners, using different DTI protocols and therefore a direct inter-group comparison among FA values is not possible.**

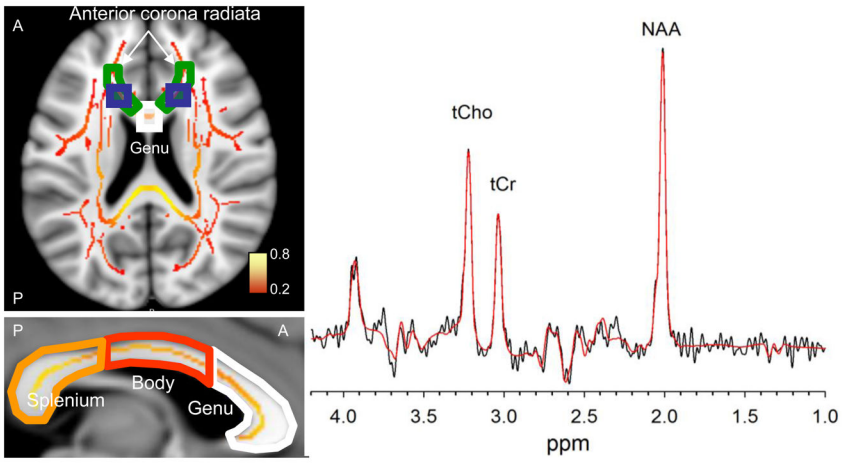

Figure 2.

Left. An axial slice (Talairach Z=10) shows the placement of bilateral spectroscopy voxels (blue boxes) with respect to the TBSS skeleton of WM tracts (average FA values color-coded from red to yellow) and two regions of interest extracted from JHU WM atlas: The genu of corpus callosum (white outline) and the anterior corona radiate (green outline). The sagittal slice through the interhemispheric fissure (Talairach X=0) shows the parcelation of corpus callosum into genu, body and splenium. Right. The representative 135-ms TE PRESS spectrum acquired from one of the voxels. Spectroscopic data from each hemisphere were fit in LCModel, and the results (red curve) were averaged after determining that the metabolite concentrations from each hemisphere were not significantly different.

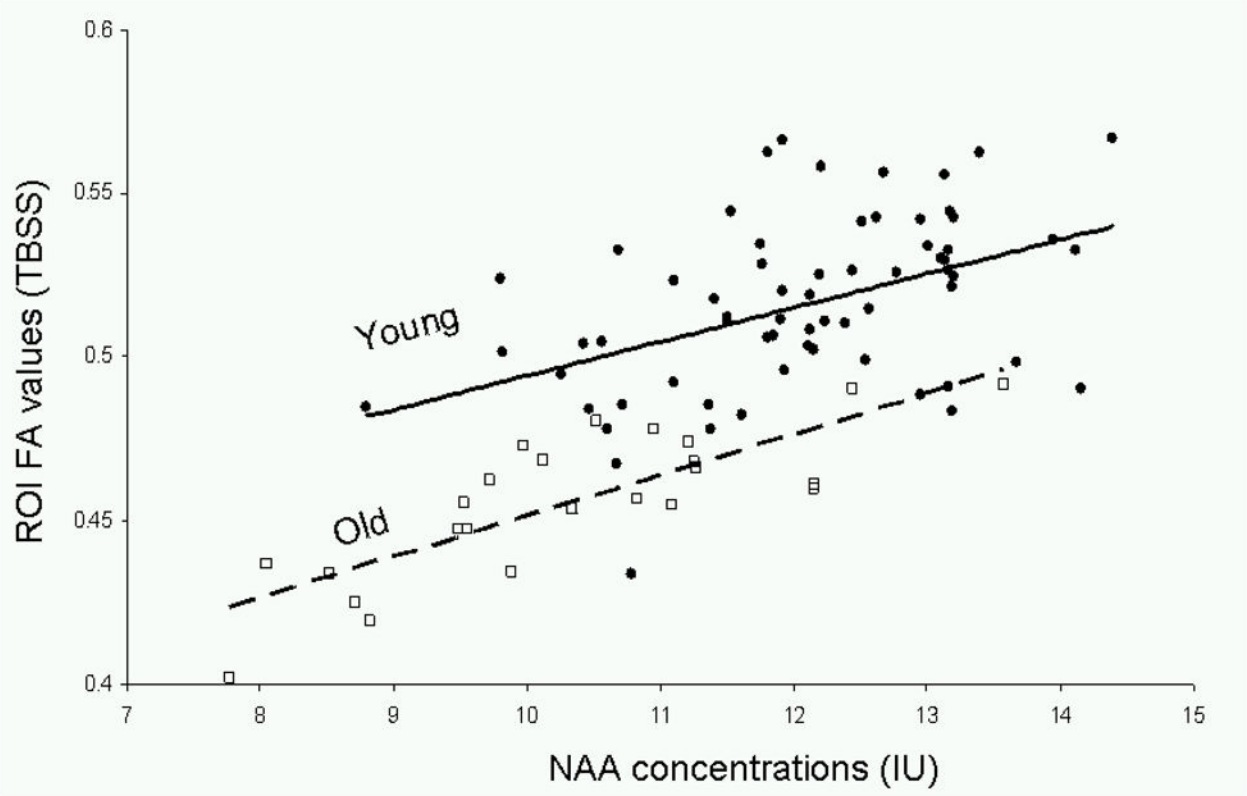

Figure 3.

FA values for the spectroscopic region of interest (sROI) and the corresponding linear trends were plotted vs. NAA concentrations in the young (solid circle markers, dashed line, FA=0.010*[NAA] + 0.39, r^2=0.21, p=0.0002) and old (hollow square markers, FA=0.013*[NAA] + 0.33, r^2=0.66, p=0.00001) cohorts.

Table 1

Summary of Parameter Means for Young Age Cohort

	Mean ± Stdev
Age	37.3 ± 6.0
Gender (M/F)	65/0
FA ROI (raw)	0.43±0.04
FA ROI (TBSS)	0.52 ± 0.03
FA ACR (TBSS)	0.51 ± 0.03
FA Genu (TBSS)	0.71 ± 0.03
FA Body (TBSS)	0.71 ± 0.05
FA Splenium (TBSS)	0.72 ± 0.03
NAA (IU)	11.8 ± 1.3
tCr (IU)	5.5 ± 0.6
tCho (IU)	2.1 ± 0.3

Table 2

Stepwise Linear Regression Results for Proximal WM tracts in the Young-Age Cohort

Outcome	Stepwise	Predictor	r^2	t	p
ROI FA (raw)		NAA	0.12	2.64	0.01 [a]
	1	tCho	-	1.04	0.31
		tCr	-	−1.43	0.15
	2	Age		.535	0.59
ROI FA (TBSS)		NAA	0.23	3.58	0.0001[a]
	1	tCho	-	−0.20	.89
		tCr	-	−0.99	0.32
	2	Age	-	0.44	0.66
ACR FA (TBSS)		NAA	0.21	3.40	0.001[a]
	1	tCho	-	−0.43	0.67
		tCr	-	−.82	0.43
	2	Age	-	0.42	0.67
Genu FA (TBSS)		NAA	0.22	2.83	0.003[a]
	1	tCho	-	1.2	0.21
		tCr	-	−0.44	0.98
	2	Age	-	−1.32	0.19

[a] $p < 0.017$

Table 3

Stepwise Linear Regression for Distal WM tracts in the Young-Age Cohort

Outcome	Stepwise	Predictor	r^2	t	p
Body FA (TBSS)	1	NAA	0.11	2.8	0.02
	2	Age	-	−0.9	0.40
Splenium FA (TBSS)	1	NAA	0.13	3.3	0.002 *a*
	2	Age	-	.61	0.54

Table 4

Summary of Parameter Means for the Old-Age Cohort

	Mean ± Stdev
Age	66.6 ± 6.2
Gender (M/F)	8/17
FA ROI (raw)	0.30 ± 0.04
FA ROI (TBSS)	0.40 ± 0.02
FA ACR (TBSS)	0.40 ± 0.03
FA Genu (TBSS)	0.56 ± 0.06
FA Body (TBSS)	0.61±0.05
FA Splenium (TBSS)	0.75±0.05
NAA (IU)	10.4 ± 1.4
tCr (IU)	5.5 ± 0.6
tCho (IU)	2.0 ± 0.4

Table 5

Stepwise Linear Regression Results for proximal WM in the Older Age Cohort

Outcome	Stepwise	Predictor	r^2	t	p
ROI FA (raw)		NAA	0.34	3.00	0.007[a]
	1	tCho	-	1.11	0.30
		tCr	-	−1.00	0.31
	2	Age		−1.10	0.31
ROI FA (TBSS)		NAA	0.66	6.50	<0.001[a]
	1	tCho	-	0.55	0.59
		tCr	-	−0.38	0.71
	2	Age	-	−0.79	0.44
ACR FA (TBSS)		NAA	0.56	5.25	<0.001[a]
	1	tCho	-	1.18	0.25
		tCr	-	−0.74	0.47
	2	Age	-	−1.07	0.30
Genu FA (TBSS)		NAA	0.28	2.96	0.007[a]
	1	tCho	-	0.86	0.399
		tCr	-	−0.22	0.826
	2	Age	-	−0.14	0.889

[a] $p < 0.017$

Table 6

Stepwise Linear Regression Results for Distal WM for the Older Age Cohort

Outcome	Stepwise	Predictor	r^2	t	p
Body FA	1	NAA	0.05	0.5	0.624
	2	Age	-	.75	0.460
Splenium FA	1	NAA	0.13	2.11	0.047
	2	Age	-	−0.18	0.890